Pervasive and diverse collateral sensitivity profiles inform optimal strategies to limit antibiotic resistance

Jeff Maltas[1] and Kevin B. Wood[1, 2, a)]

[1)] *Department of Biophysics, University of Michigan, Ann Arbor, MI 48109*

[2)] *Department of Physics, University of Michigan, Ann Arbor, MI 48109*

The growing threat of drug resistance has inspired a surge in evolution-based strategies for optimizing the efficacy of antibiotics. One promising approach involves harnessing collateral sensitivity–the increased susceptibility to one drug accompanying resistance to a different drug–to mitigate the spread of resistance. Unfortunately, because the mechanisms of collateral sensitivity are diverse and often poorly understood, the systematic design of multi-drug treatments based on these evolutionary trade-offs is extraordinarily difficult. In this work, we provide an extensive phenotypic characterization of collateral drug effects in *E. faecalis*, a gram positive species among the leading causes of nosocomial infections. By combining parallel experimental evolution with high-throughput dose-response measurements, we provide quantitative profiles of collateral sensitivity and resistance for a total of 900 mutant-drug combinations. We find that collateral effects are pervasive but difficult to predict, as even mutants selected by the same drug can exhibit qualitatively different profiles of collateral sensitivity. Remarkably, however, the sensitivity profiles cluster into statistically similar groups characterized by selecting drugs with similar mechanisms. To exploit the underlying statistical structure in the collateral profiles, we develop a simple mathematical framework based on a Markov decision process (MDP) to identify optimal antibiotic cycling policies that maximize expected collateral sensitivity. Importantly, these cycles can be tuned to optimize long-term treatment outcomes, leading to drug sequences that may produce long-term collateral sensitivity at the expense of short-term collateral resistance.

[a)] Electronic mail: kbwood@umich.edu

I. INTRODUCTION

The rapid emergence of drug resistance is an urgent threat to effective treatments for bacterial infections, cancers and many viral infections[1–6]. Unfortunately, the development of novel drugs is a long and arduous process, underscoring the need for alternative approaches to forestall resistance evolution. Recent work has highlighted the promise of evolution-based strategies for optimizing and prolonging the efficacy of established drugs, including optimal dose scheduling[7–9], antimicrobial stewardship[10,11], drug cycling[12–14], consideration of spatial dynamics[15,16], cooperative dynamics[17–20], or phenotypic resistance[21–23], and judicious use of drug combinations[24–31]. In a similar spirit, a number of recent studies have suggested exploiting collateral sensitivity as a means for slowing or even reversing antibiotic resistance[32–35]. Collateral evolution occurs when a population evolves resistance to a target drug while simultaneously exhibiting increased sensitivity or resistance to a different drug. From an evolutionary perspective, collateral effects are reminiscent of the trade-offs inherent when organisms are required to simultaneously adapt to different tasks, an optimization that is often surprisingly simple because it takes place on a low-dimensional phenotypic space[36,37]. If similarly tractable dynamics occur in the evolution of multi-drug resistance, systematic optimization of drug deployment has the promise to mitigate the effects of resistance.

Indeed, recent studies in bacteria have shown that the cyclic[38–40] or simultaneous[41] deployment of antibiotics with mutual collateral sensitivity can sometimes slow the emergence of resistance. Unfortunately, collateral profiles have also been shown to be highly heterogeneous[42,43] and often not repeatable[44], potentially complicating the design of successful collateral sensitivity cycles. The picture that emerges is enticing, but complex; while collateral effects offer a promising new dimension for optimizing therapies, the ultimate success of these approaches will require quantitative and predictive understanding of both the prevalence and repeatability of collateral sensitivity profiles across species.

In this work, we provide an extensive quantitative look at collateral drug effects in *E. faecalis*, a gram-positive species often implicated in nosocomial infections, including bacteremia, native and prosthetic valve endocarditis, and medical device infections[45–48]. By combining parallel experimental evolution of *E. faecalis* with high-throughput dose-response measurements, we provide collateral sensitivity and resistance profiles for 60 strains evolved to 15 different antibiotics, yielding a total of 900 mutant-drug combinations. We find that col-

lateral resistance and collateral sensitivity are pervasive in drug-resistant mutants, though patterns of collateral effects can vary significantly, even for mutants evolved to the same drug. Remarkably, however, the sensitivity profiles cluster into groups characterized by selecting drugs from similar drug classes, indicating the existence of large scale statistical structure in the collateral sensitivity network. Finally, we develop a simple mathematical framework based on Markov Decision Processes (MDP) to identify optimal antibiotic cycling policies that maximize expected collateral sensitivity. These cycles can be tuned to optimize either short-term or long-term evolutionary outcomes and yield strikingly different protocols depending on the time horizon for treatment.

II. RESULTS

A. Collateral effects are pervasive and heterogeneous

To investigate collateral drug effects in *E. faecalis*, we exposed four independent populations of strain V583 to increasing concentrations of a single drug over 8 days (approximately 60 generations) using serial passage laboratory evolution (Figure 1A, Methods). We repeated this evolution for a total of 15 commonly used antibiotics spanning a wide range of clinically relevant classes and mechanisms of action (Table 1). After approximately 60 generations, we isolated a single colony from each population and measured its response to all 15 drugs using replicate dose-response experiments (Figure 1B). To quantify resistance, we estimated the half maximal inhibitory concentration (IC_{50}) for each mutant-drug combination using nonlinear least squares fitting to a Hill-like dose response function (Methods; see Figure S1 for examples). A mutant strain was deemed collaterally sensitive (resistant) to an antibiotic if its IC_{50} decreased (increased) by more than $3\sigma_{WT}$, where σ_{WT} is the uncertainty (standard error across replicates) of the IC_{50} measured in the wild-type strain. As a measure of collateral resistance / sensitivity, we then calculate $C \equiv \log_2 (\mathrm{IC}_{50,Mut}/\mathrm{IC}_{50,WT})$, the (log-scaled) fold change in IC_{50} of each mutant relative to wild-type (WT); values of $C > 0$ indicate collateral resistance, while values of $C < 0$ indicate collateral sensitivity (Figure 1C). For each mutant, we refer to the set of 15 C values (one for each testing drug) as its collateral sensitivity profile $\bar{C}$.

Our results indicate that collateral effects–including sensitivity–are pervasive, with ap-

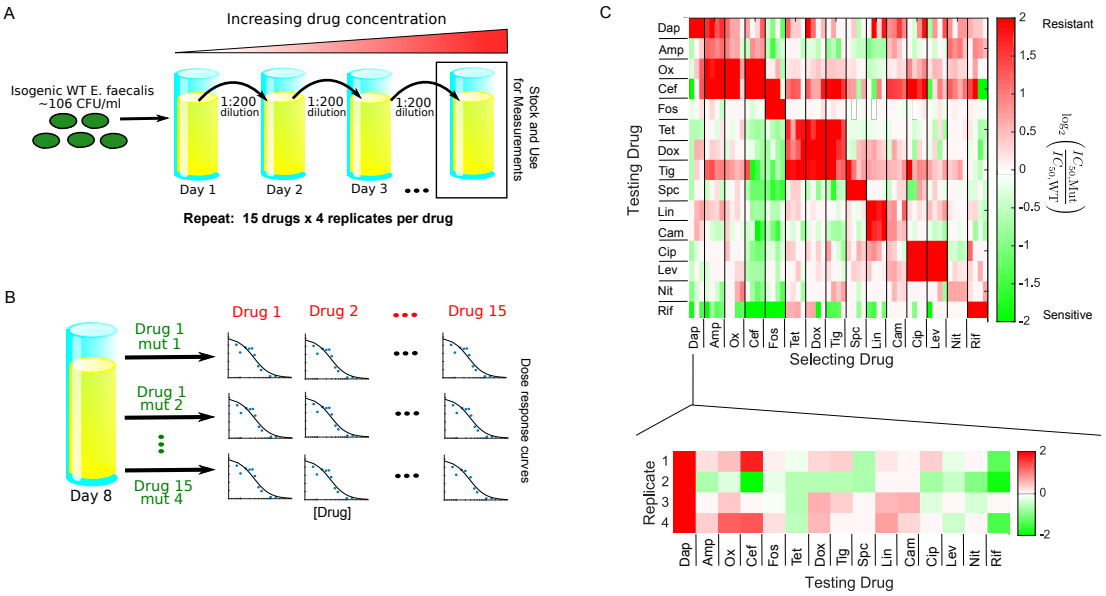

FIG. 1. **Collateral effects are pervasive and vary across parallel evolution experiments in *E. faecalis*.** A. *E. faecalis* strain V583 was exposed to increasing concentrations of a single antibiotic over an 8-day serial passage experiment with daily 200-fold dilutions (≈60 generations total; see Methods). The evolution was performed in quadruplicate for each drug and repeated for a total of 15 drugs. After 8 days, a single mutant was isolated from each population. B. The half maximal inhibitory concentration (IC_{50}) for each of 15 drugs was estimated for all 60 mutants by nonlinear fitting of a dose response curve (relative OD) to a Hill-like function (Methods). C. Main panel: resistance (red) or sensitivity (green) of each evolved mutant (horizontal axis; 15 drugs x 4 mutants per drug) to each drug (vertical axis) is quantified by the $\log_2$-transformed relative increase in the IC_{50} of the testing drug relative to that of wild-type (V583) cells. While the color scale ranges from a 4x decrease to a 4x increase in IC_{50}, it should be noted that both resistance to the selecting drug (diagonal blocks) and collateral effects can be significantly higher. Each column of the heat map represents a collateral sensitivity profile for one mutant. Bottom panel: enlarged (and rotated) column from main panel. Mutants isolated from replicate populations evolved to daptomcyin exhibit diverse sensitivity profiles. While all mutants are resistant to the selecting drug (daptomycin), mutants may exhibit either sensitivity or resistance to other drugs. For example, replicates 1 and 4 exhibit collateral resistance to ceftriaxone (cef), while replicate 2 exhibits collateral sensitivity and replicate 3 shows little effect.

proximately 73 percent (612/840) of all (collateral) drug-mutant combinations exhibiting a statistically significant change in IC_{50}. The mutants in our study exhibit collateral sensitivity to a median of 4 drugs, with only 3 of the 60 mutants (5 percent) exhibiting no collateral sensitivity at all; by contrast, mutants selected by ceftriaxone (cef) and fosfomycin (fos) exhibit particularly widespread collateral sensitivity. Collateral resistance is similarly prevalent, with only 2 strains failing to exhibit collateral resistance to at least one drug. Somewhat surprisingly, 56 of 60 mutants exhibit collateral resistance to at least one drug from a different class (e.g. all mutants evolved to ciprofloxacin, a DNA synthesis inhibitor, show increased resistance ceftriaxone, an inhibitor of cell wall synthesis).

In addition, collateral effects can be quite large. For example, we measure 8 instances of collateral sensitivity where the IC_{50} decreases by 16 fold or more. We also observe a strong, repeatable collateral sensitivity to rifampicin when mutants were selected by inhibitors of cell wall synthesis, an effect that–to our knowledge–has not been reported elsewhere. More typically, however, collateral effects are smaller than the direct effects to the selecting drug, with 46 percent (384/840) exhibiting more than a factor 2 change in IC_{50} and only 7 percent (61/840) exhibiting more than a factor 4 change.

B. Variation in collateral profiles is correlated with resistance to selecting drug and prevalence of large collateral effects to testing drug.

Our results also indicate that collateral profiles can vary significantly even when mutants are evolved in parallel to the same drug (Figure 1C). For example, all 4 mutants selected by daptomycin exhibit high-level resistance to the selecting drug, but replicates 1 and 4 exhibit collateral resistance to ceftriaxone (cef), while replicate 2 exhibits collateral sensitivity and replicate 3 shows little effect (Figure 1C, bottom panel).

To quantify the variation between replicates selected by the same drug, we viewed the collateral profile of each mutant (i.e. a column of the collateral sensitivity matrix in Figure 1) as a vector in 15-dimensional drug resistance space. Then, for each set of replicates, we defined the variability $V \equiv \sum_{i=1}^{m} d_i/m$, where $m = 4$ is the number of replicates and d_i is the Euclidean distance between mutant i and the centroid formed by all vectors corresponding to a given selecting drug (Figure 2A). Variability differs for different selecting drugs, with daptomycin and rifampicin showing the largest variability and nitrofurantoin the smallest (Figure 2B). Interestingly, we find that the observed variability is significantly correlated with average resistance to the selecting drug (Figure S2). This correlation persists even when one removes contributions to variability from the selecting drug (Figure 2C), indicating that collateral (rather than direct) effects underlie the correlation. We do note, however, that selection by spectinomcyin represents a notable exception to this trend.

While resistance to the selecting drug is correlated with profile variability, it is not clear whether a similar relationship exists between repeatability (across replicates) and certain testing drugs. To investigate this question, we calculated the variance of C (see Figure 1C) across replicates for each combination of selecting and testing drug (Figure 2D). We find that

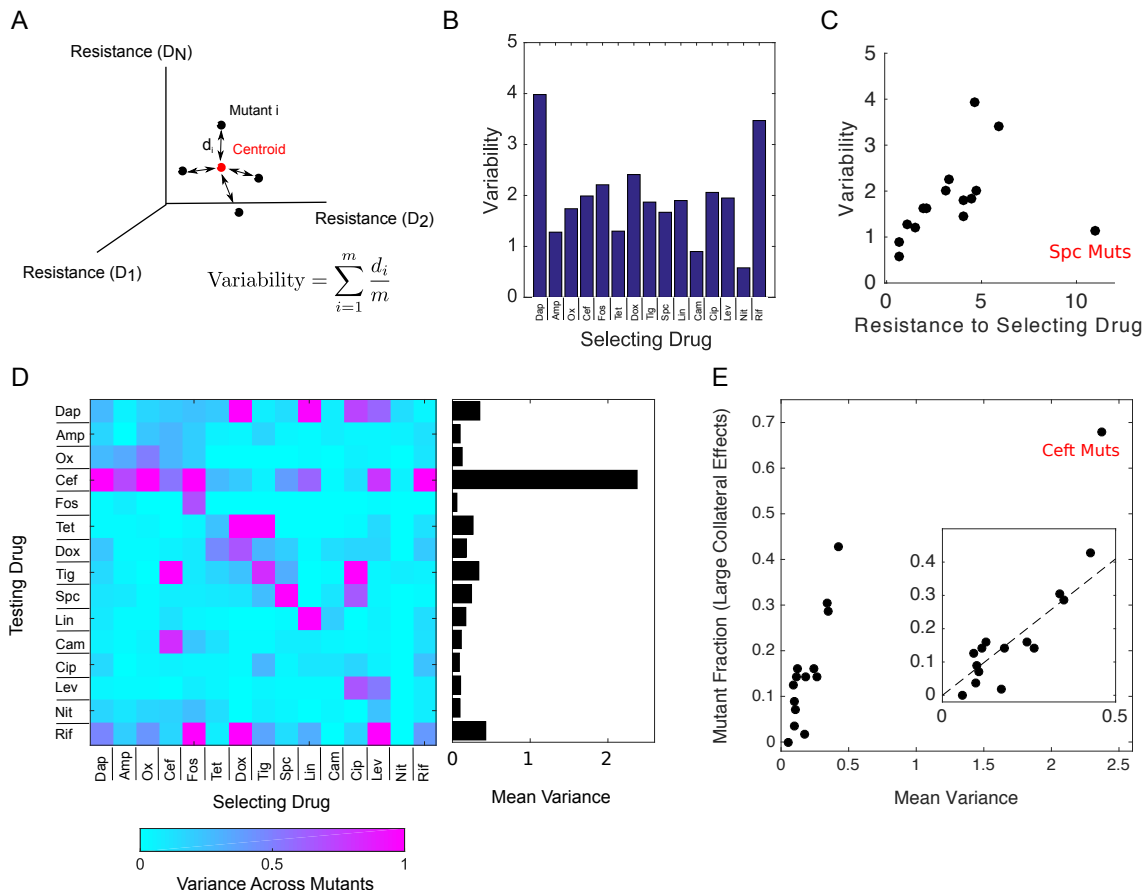

FIG. 2. **Variation in collateral profiles is correlated with resistance to selecting drug and prevalence of large collateral effects to testing drug.** A. Variability in collateral profiles between mutants selected by the same drug is defined by first representing each mutant's collateral profile as a vector $\bar{C}$ in 15-dimensional drug space. Dimension i represents the $\log_2$-scaled fold increase in IC_{50} (relative to wild-type) for drug i. The variability for a set of mutants evolved to the same drug is then given by the average Euclidean distance d_i for a mutant from the centroid. B. Variability in replicates (defined in panel A) for all 15 drugs used for selection. C. Scatter plot between the variability calculated in (B)–now with effects of selecting drug removed–and the ($\log_2$-scaled) fold increase in IC_{50} to the selecting drug (Spearman correlation of 0.58, $p = 0.03$ including the spc mutants; 0.82, $p < 10^{-3}$ without the spc mutants.). To remove effects from the selecting drug, variability is calculated in the 14-dimensional space defined by removing the selecting drug. D. Main panel: heatmap of variance in resistance level ($\log_2$-scaled fold increase in IC_{50} relative to wild-type) across populations selected by the same drug. Right panel: mean variance to each selecting drug (mean across rows in heatmap). E. Scatter plot between mean variance (calculated in D) and the fraction of all mutants exhibiting large collateral effects. A large collateral effect is defined to be a change in resistance to a non-selecting drug leading to a greater than 2-fold change in IC_{50} (Spearman correlation 0.84). Inset: expanded view of main plot. Dashed line: best linear fit (excluding ceftriaxone mutants).

the majority of the variance values are less than 0.5, through rare instances of larger variance occur. To determine whether variance is related to the drug used for testing, we calculated the mean variance across all selecting drugs (Figure 2D, right panel). Interestingly, the average variance for some drugs (most notably ceftriaxone) is considerably higher than for others (e.g. fosfomycin), and this variance is strongly correlated with the prevalence of large collateral effects (i.e. the fraction of mutants exhibiting greater than 2-fold change in IC_{50}). Notably, however, the collateral effects to ceftriaxone and fosfomycin are qualitatively (direction-wise) almost identical, despite the large differences in magnitude.

Overall, these results suggest that the repeatability of collateral effects is sensitive to both the drug used for selection and the drug used for testing. As a result, certain drugs may be more appropriate for establishing robust antibiotic cycling profiles.

C. Collateral Resistance Threatens the Efficacy of Daptomycin

Daptomycin is a lipopeptide antibiotic that is often used as a last line of defense against gram-positive bacterial infections, including vancomycin resistant enterococcus (VRE). While daptomycin resistance was initially believed to be quite rare[49], it has become increasingly documented in clinical settings[50]. Given the clinical importance of daptomycin, it is perhaps surprising that resistance to daptomycin is particularly common when populations are selected by other antibiotics. Specifically, we found that 66 percent of all evolved lineages display collateral resistance to daptomycin, while only 9 percent of lineages display collateral sensitivity (Figure 3A).

D. Selection by linezolid enhances resistance to chloramphenicol

Surprisingly, we found that mutants selected by linezolid (lin) developed higher resistance to chloramphenicol (cam) than mutants selected directly by cam (Figure 3B). To investigate this phenomenon, we isolated linezolid-selected mutants at days 2, 4, 6 and 8 of the laboratory evolution and measured the resistance of each to chloramphenicol. Interestingly, we see that early-stage (days 4-6) mutants exhibit low level chloramphenicol sensitivity just prior to a dramatic increase in collateral resistance around day 8. These findings suggest linezolid selection drives the population across a chloramphenicol fitness valley, ultimately

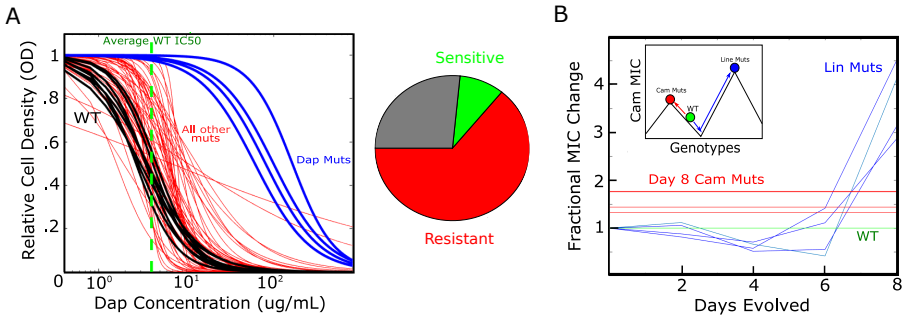

FIG. 3. **Collateral resistance threatens the efficacy of daptomycin and can magnify resistance to chloramphenicol.** A. Estimated dose response curves (fit to Hill-like function) for all mutants tested against daptomycin. Strains evolved to daptomycin (blue) and all other drugs (red) frequently exhibit increased resistance to daptomycin relative to wild-type (black, individual replicates; dotted green line, mean IC_{50}). Right inset: Approximately 66 percent of all drug-evolved mutants exhibit increased daptomycin resistance, while only 9 percent exhibit collateral sensitivity. B. Fractional change in chloramphenicol (cam) IC_{50} for mutants evolved to linezolid (blue). The width of the green line represents the confidence interval ($\pm$ 3 standard errors of the mean measured over 8 replicate measurements) for the (normalized) choramphenicol IC_{50} in wild-type cells. For comparison, the red lines represent the final (day 8) cam resistance achieved in populations evolved directly to cam. Inset: Schematic depicting two paths to different cam resistance maximums. The green circle represents the sensitive wild-type. Evolution can occur to cam directly (red line) or to cam collaterally through lin resistance (blue line). The lin evolution depicts early collateral sensitivity before ultimately achieving a higher total resistance.

leading to levels of resistance that exceed those observed by direct chloramphenicol selection (Figure 3B, inset). While temporally dynamic collateral responses have been recently measured in cancer[43,51], this represents, to our knowledge, the first evidence of temporally dynamic collateral responses in bacteria.

E. Sensitivity profiles cluster into groups based on known classes of selecting drug

Our results indicate that there is significant heterogeneity in collateral sensitivity profiles, even when parallel populations are selected on the same antibiotic. While the genetic networks underlying these phenotypic responses are complex and, in many cases, poorly understood, one might expect that selection by chemically or mechanistically similar drugs would lead to profiles with shared statistical properties. For example, previous work showed

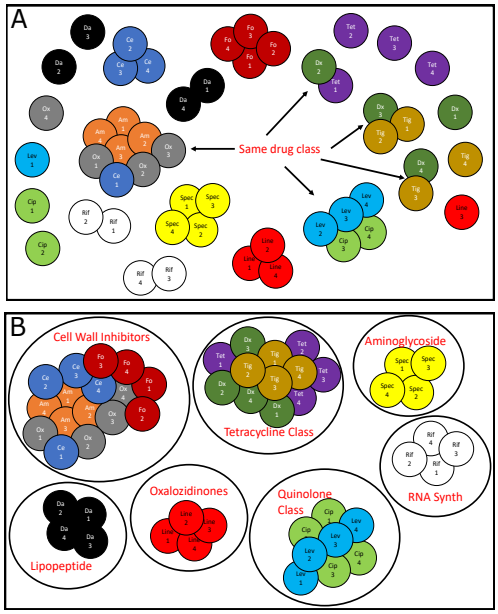

FIG. 4. **Hierarchical clustering of collateral sensitivity profiles partitions mutants into groups selected by known drug classes** A. Each circle represents a single mutant. Color depicts drug used for selection. Low-level clustering is largely characterized by grouping of mutants evolved to the same drug (i.e. replicate evolution experiments). However, in several cases mutants selected by one drug (e.g. tigecycline, Tig) cluster with mutants selected by a different drug (doxycycline, Dx) of the same class. B. At later stages of clustering, mutants evolved to drugs from a similar class–or with similar mechanisms of action– tend to cluster together.

(in a different context) that pairwise interactions between simultaneously applied antibiotics can be used to cluster drugs into groups that interact monochromatically with one another; strikingly, these groups correspond to known drug classes[52], highlighting statistical structure in drug interaction networks that appear, on the surface, to be extremely heterogeneous. Similarly, we asked whether collateral sensitivity profiles can be used to cluster resistant mutants into statistically similar classes. To answer this question, we performed hierarchical clustering on collateral sensitivity profiles for all mutants (52 total) that achieved high-level resistance (at least a mean 2-fold increase in IC_{50}) to the selecting drug (Methods; Note that we excluded mutants selected by Cam and Nitro, which did not achieve high-level resistance, but we repeated the analysis with those drugs included in Figure S3). Initially, mutants selected by the same drugs or by drugs within the same drug class (e.g. Dox and Tet, Dox and Tig, Lev and Cip, etc) cluster together (Figure 3A; Figure S4 for dendograms), Strikingly, despite the heterogeneity in collateral profiles, the clustering eventually partitions

mutants into groups characterized–almost exclusively–by selecting drugs from established drug classes. For example, inhibitors of cell wall synthesis (amp, ceft, fos, ox) cluster into one group, while tetraclycine-like drugs (tet, dox, tig) cluster into another. At the same time, this analysis does separate some drugs with similar mechanisms (e.g. tetracycline and spectinomycin, both of which target the 30S ribosomal subunits), and it therefore may help identify mechanistically similar drugs likely to generate statistically distinct sensitivity profiles.

F. A Markov decision process (MDP) model predicts optimal drug policies

Our results indicate that collateral sensitivity is pervasive, and while collateral sensitivity profiles are highly heterogeneous, clustering suggests the existence of statistical structure in the data. Nevertheless, because of the stochastic nature of the sensitivity profiles, it is not clear how to best utilize this information to design optimal treatment protocols. To address this problem, we develop a simple mathematical model based on a Markov decision process (MDP) to predict optimal drug cycles. MDP's are widely used in applied mathematics and finance and have a well-developed theoretical basis[53]. In a MDP, a system transitions stochastically between discrete states. Each state is assigned a particular "cost" (or value), and at each time step, we must make a decision (called an "action") that potentially influences which state will occur next. The goal of the MDP is develop a policy–a set of actions corresponding to each state–that will optimize some objective function (e.g. minimize the expected cost) over some time period.

For our system, the state s_{t_i} at time step $t_i = 0, 1, 2, ...$ is defined by the collateral sensitivity profile $\bar{C}$ describing the current (mutant) population as well as the current drug, D_{t_i}. As in the previous section, we exclude mutants selected by Cam and Nit, which did not achieve high-level resistance to the selecting drug and may therefore be preferentially (and trivially) selected by the optimization algorithm. At each time step, an action a_{t_i} is chosen that determines the drug used at the next time step, $a_{t_i} \to D_{t_{i+1}}$. The system–which is assumed to be Markovian–then transitions with probability $P(s_{t_{i+1}}|s_{t_i}, a_{t_i})$ to a new state $s_{t_{i+1}}$, and the transition probabilities are estimated from evolutionary experiments (or any available data). The cost function $r_{t_i} \equiv r_{t_i}(s_{t_i})$ defines a cost associated with each state and can be chosen to represent–for example–the level of collateral sensitivity of the current

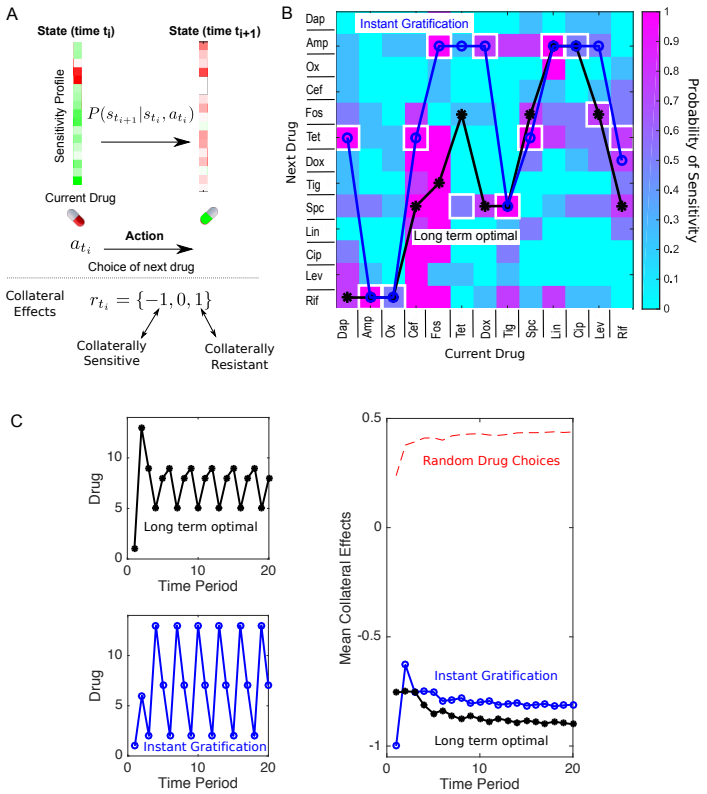

FIG. 5. **Drug sequences can be chosen to maximize collateral sensitivity over different timescales.** A. Schematic: markov decision process (MDP) for maximizing collateral sensitivity. The state s_{t_i} at time step t_i is defined by the sensitivity profile of the current mutant and the current drug. The action a_{t_i} that determines the drug at the next time step. The system transitions between states according to the conditional probability $P(s_{t_i+1}|s_{t_i}, a_{t_i})$, which is estimated from lab evolution experiments (e.g. Figure 1). The cost function r_{t_i} at time t_i is either -1, 0, or 1 depending on whether the sensitivity profile shows sensitivity, no effect, or resistance, respectively, to the current drug. The optimal policy Π is chosen to minimize $R(s) \equiv \langle \sum_{t_i=1}^{\infty} \gamma^{t_i} r_{t_i} \rangle$, where brackets indicate an expectation value conditioned on the initial state s_0 and the choice of policy Π. The parameter $0 \leq \gamma < 1$ is a discount factor that determines the timescale for the optimization. B. Heat map indicates the probability of collateral sensitivity to the next drug (rows) given a particular selecting drug (columns). Black stars: optimal short term policy (instant gratification; $\gamma = 0$)); blue circles: optimal long-term policy ($\gamma = 0.95$). White squares indicate maximum of each column. C. Left panels: optimal drug cycles, starting from drug 1 (Dap), for long term (upper panel) and instant gratification (lower panel) strategies. Long-term strategy asymptotically approaches a cycle between drugs 5 (Fos), 8 (Tig), and 9 (Spc); the instant gratification strategy approaches a cycle between drug 2 (Amp), 13 (Rif), and 7 (Dox). Right panel: mean collateral effects (cumulative) for the long-term strategy (black), instant gratification strategy (blue), and random drug cycles (red, dashed). The mean collateral effect at time step t_i is given by $\langle \sum_{t=1}^{t_i} \frac{r_t}{t} \rangle$, where brackets indicate an average over 1000 independent simulations of the MDP. Here r_t is -1, 0, or 1 if the profile at the current time step is sensitive to, not affected by, or resistant to the current drug, respectively.

mutant to the current drug. The optimal policy Π is a mapping $\Pi : s_{t_i} \rightarrow a_{t_i}$ from each state to the optimal action (i.e. the optimal next drug). The policy is chosen to minimize $R(s) \equiv \langle \sum_{t_i=0}^{\infty} \gamma^{t_i} r_{t_i} \rangle$, where brackets indicate an expectation value conditioned on the initial state s_0 and the choice of policy Π. The parameter $\gamma < 1$ is a discount factor that determines the timescale for the optimization; $\gamma \approx 1$ leads to long-time optimal solution, while $\gamma \approx 0$ leads to solutions that maximize near-term success.

To apply the MDP framework to collateral sensitivity profiles, we must infer from our data a set of (stochastic) rules for transitioning between states (i.e. we must estimate $P(s_{t_{i+1}}|s_{t_i}, a_{t_i})$). While many choices are possible–and these choices may be refined as additional data is collected–in what follows we consider a simple model where the system can transition only to a state corresponding to one of the four sensitivity profiles experimentally measured under selection to the current drug D_{t_i} (but see Figure S5 and Figure S6 for similar calculations using a model where transitions can occur to *any* sensitivity profile with resistance to the current drug). For example, if the current drug is daptomycin, the sensitivity profile at the next step will be chosen (with uniform probability) to be one of those measured for the four replicates selected by daptomycin (see Figure 1C, bottom panel). Each time step is therefore assumed to cover approximately 60 generations, similar to the evolution time in our experiments. In addition, this model implicitly assumes sufficiently strong selection that, at each step, the state of the system is fully described by a single collateral sensitivity profile (rather than, for example, a heterogeneous ensemble of profiles that would be required to model clonal interference).

To maximize the effect of collateral sensitivity, we first choose the cost function r_{t_i} to be -1, 0, or 1 if the profile at the current time step is sensitive to, not affected by, or resistant to the current drug, respectively. Intuitively, the goal is to reward drug choices that lead to sensitivity while punishing those associated with resistance. Interestingly, the drug policy Π that minimizes $R(s)$ varies significantly depending on the value of γ–that is, on the timescale of the optimization (Figure 5B). The "instant gratification" policy ($\gamma = 0$) optimizes short term success and therefore tends to maximize the probability of achieving collateral sensitivity at the next time step (Figure 5B, blue circles; Note that because the MDP minimizes cost rather than maximizing probability of sensitivity, even the short-term solution does not always maximize the probability of sensitivity at the next step). On the other hand, the longer term optimization ($\gamma = 0.95$) may forgo short-term success for longer-term gain.

For example, if the population is currently exposed to daptomycin, the instant gratification policy prescribes tetracycline as the next drug, which maximizes the probability of collateral sensitivity (i.e. all four mutants selected by daptomycin were sensitive to tetracycline). On the other hand, the long-term optimal policy prescribes rifampicin as the next drug, even though the probability of sensitivity to rifampicin is lower.

G. Optimal drug cycles depend on timescale for optimization process

Once an optimal policy has been found, one can consider a treatment starting from any drug and iteratively determine the sequence of drugs that should follow. Consider a treatment that starts with daptomycin (drug 1). The instant gratification policy leads to a drug sequence of daptomycin (1), tetracycline (6), ampicillin (2), rifampicin (13), and doxycyline (7) before settling into a long-term cycle between the latter 3 drugs (Figure 5C, lower left panel). By contrast, the long-term policy leads to a sequence of daptomycin (1) and rifampicin (13) before settling into a long-term cycle between spectinomycin (9), fosfomycin (5), and tigecycle (8) (Figure 5C, upper left panel). To compare the expected results of both policies, we simulated the MDP and calculated the mean (cumulative) collateral effect at time step t_i, which is given by $\langle \sum_{t=0}^{t_i} \frac{r_t}{t+1} \rangle$, where brackets indicate an average over 1000 independent simulations of the MDP. While both policies perform significantly better than random drug cycling, the long-term solution leads to the most collateral sensitivity on longer time scales, despite performing worse than the instant gratification on the first time step (Figure 5C, right panel).

H. Optimal cycles do not always involve drugs with mutual collateral sensitivity

The cost function in the previous section was chosen to reward collateral sensitivity and punish collateral resistance, but it did not account for the magnitude of the effects. To incorporate these magnitudes, we repeated the MDP analysis with r_{t_i} chosen to be the value C of the collateral profile against the current drug. As before, the instant gratification ($\gamma = 0$) strategy led to a different policy and, in turn, to different optimal cycles than the long-term optimization ($\gamma = 0.95$). While the instant gratification strategy leads to a long-term

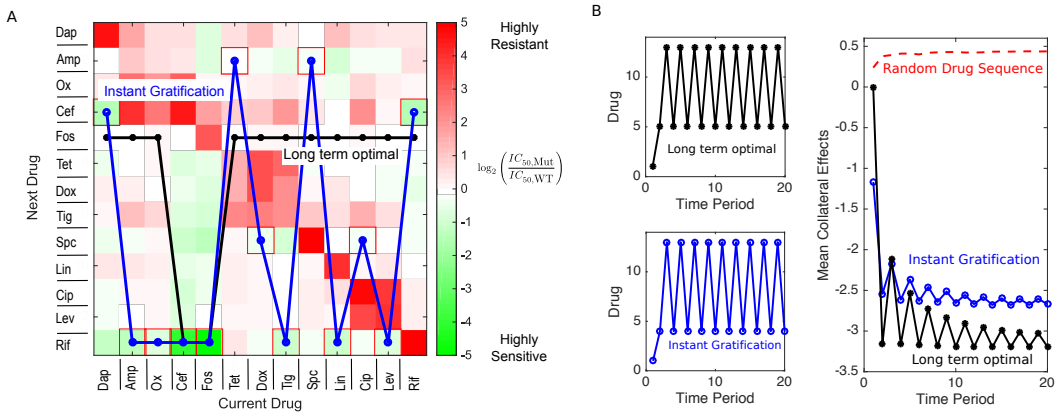

FIG. 6. **Maximizing collateral sensitivity values may lead to cycles between drugs without mutual collateral sensitivity.** A. Heat map indicates the mean value (over replicates) of collateral sensitivity to the next drug (rows) given a particular selecting drug (columns). Black stars: optimal short term policy (instant gratification; $\gamma = 0$)); blue circles: optimal long-term policy ($\gamma = 0.95$). Red squares indicate minimum of each column. Note that the scale is much larger than in Figure 1 to highlight large sensitivity values relevant for drug cycles. B. Left panels: optimal drug cycles, starting from drug 1 (Dap), for long term (upper panel) and instant gratification (lower panel) strategies. Long-term strategy asymptotically approaches a cycle between drugs 5 (Fos) and 13 (Rif); the instant gratification strategy approaches a cycle between drugs 4 (Cef) and 13 (Rif). Right panel: mean collateral effects (cumulative) for the long-term strategy (black), instant gratification strategy (blue), and random drug cycles (red, dashed). The mean (cumulative) collateral effect at time step t_i is given by $\langle \sum_{t=0}^{t_i} \frac{r_t}{t+1} \rangle$, where brackets indicate an average over 1000 independent simulations of the MDP. Here r_t is the value C of collateral sensitivity or resistance to the current drug.

cycle between drugs with–on average–mutual collateral sensitivity (Figure 6; ceft (4) and rifampicin (13)), the long-term policy involves a cycle between fosfomycin (5) and rifampicin (13), despite the fact that mutants selected by rifampicin do not show appreciable collateral sensitivity to fosfomycin. Intuitively, the long-term optimal makes a single sub-optimal step (rifampicin → fosfomycin)–and one that can sometimes lead to collateral resistance– because the long term cycle between the two drugs is dominated by the large collateral sensitivity imparted by the reverse step (fosfomycin → rifampicin; Figure 5B, right panel).

III. DISCUSSION

Our work provides an extensive quantitative study of phenotypic collateral drug effects in *E. faecalis*. We have shown that collateral resistance and collateral sensitivity are widespread but heterogeneous, with patterns of collateral effects often varying even between mutants evolved to the same drug. Our results contain a number of surprising, drug-specific observations; for example, we observed a strong, repeatable collateral sensitivity to rifampicin when mutants were selected by inhibitors of cell wall synthesis. Additionally, cross-resistance to daptomycin, often viewed as a last line of defense for dangerous clinical infections, is particularly common when cells are selected by other frequently used antibiotics. Because the FDA/CLSI breakpoint for daptomycin resistance is not dramatically different than the MIC distributions found in clinical isolates prior to daptomycin use[54], one may speculate that even small collateral effects could have potentially harmful consequences for clinical treatments involving daptomycin. In addition, we found that selection by one drug (linezolid) led to higher overall resistance to chloramphenicol than direct selection by chloramphenicol, illustrating how indirect selection may drive a population across a fitness valley to an otherwise inaccessible fitness peak.

Our findings also point to global trends in collateral sensitivity profiles. For example, we found that the repeatability of collateral effects is sensitive to both the drug used for selection and the drug used for testing, meaning that some drugs may be better than others for establishing robust antibiotic cycling profiles. On the other hand, despite the apparent unpredictability of collateral effects at the level of individual mutants, the sensitivity profiles for mutants selected by drugs of a similar class or mechanism cluster into statistically similar groups. This clustering process may be useful, in principle, for identifying novel classes of chemotherapeutic agents with favorable sensitivity profiles. Finally, we show how these profiles can be incorporated into a rigorous MDP framework that optimizes drug cycling protocols while accounting for effects of both stochasticity and different time horizons. Within this framework, cycling protocols can be tuned to optimize either short-term or long-term evolutionary outcomes, leading to dramatically different drug sequences.

Our results complement recent studies on collateral sensitivity and also raise a number of new questions for future work. First, several previous studies have indicated that cycles involving mutually collaterally sensitive drugs may be chosen to harness collateral sensitiv-

ity and minimize the evolution of resistance[38,39]. In the context of our MDP model, these cycles would correspond to a type of short-time-horizon optimization similar to our "instant gratification" strategy. Interestingly, however, our results indicate that considering longer time horizons can lead to cycles involving at least one sub-optimal step, including one to a collaterally resistant state. In addition, recent work has highlighted that collateral profiles are heterogeneous[42,43], and optimization will therefore require incorporation of stochastic effects such as likelihood scores[44]. These likelihood scores could potentially inform transition probabilities in our MDP approach, leading to specific predictions for optimal drug sequences.

Overall, the success of the approach will rely on robust inference of clinically-relevant model parameters–such as transition probabilities–and a careful choice of an appropriate cost function. While in vitro models of pharmacodynamics are often used to inform clinical protocols, it is not clear that in vivo evolutionary trajectories will mimic, in any way, the highly controlled evolution in laboratory environments. Nevertheless, while the current proof-of-principle model is clearly an oversimplification of the evolutionary process, it can be readily expanded to account for more realistic scenarios and to incorporate more complex data sets. Most notably, collateral sensitivity profiles in cancer have been previously shown to be time-dependent[43,51]; our future work will focus on characterizing dynamic properties of collateral effects in *E. faecalis* and expanding the MDP approach to account for time-varying sensitivity profiles. It may also be interesting to investigate collateral effects in *E. faecalis* biofilms, where some classes of antibiotics can have counterintuitive effects even on evolutionarily short timescales[55]. On longer timescales, elegant experimental approaches to biofilm evolution have revealed that spatial structure can give rise to rich evolutionary dynamics[56,57], though to date, little is known about collateral drug effects in these systems.

Our results also raise questions about the potential molecular and genetic mechanisms underlying the observed collateral effects. While the clustering analysis presented here may point to shared mechanistic explanations for sensitivity profiles selected by similar drugs, uncovering the detailed genetic underpinnings of collateral sensitivity remains an ongoing challenge for future work. At the same time, because our results are based on phenotypic measurements, they may allow for systematic optimization of drug cycling protocols even when molecular mechanisms are not fully known.

IV. MATERIALS AND METHODS

A. Strains, antibiotics and media

All resistant lineages were derived from *E. faealis* V583, a fully sequences vancomycin-resistant clinical isolate[58]. The 15 antibiotics used are listed in Table 1. Each antibiotic was prepared from powder stock and stored at -20°C with the exception of ampicillin, which was stored at -80°C. Evolution and IC_{50} measurements were conducted in BHI medium alone with the exception of daptomycin, which requires an addition of 50 mM calcium for antimicrobial activity.

B. Laboratory Evolution Experiments

Evolution experiments to each antibiotic were performed in quadruplicate. Evolutions were performed using 1 mL BHI medium in 96-well plates with maximum volume 2 mL. Each day, populations were grown in at least three different antibiotic concentrations spanning both sub- and super-MIC doses. After 16-20 hours of incubation at 37°C, the well with the highest drug concentration that contained visual growth was propagated into 2 higher concentrations (typically a factor 2x and 4x increase in drug concentration) and 1 lower concentration to maintain a living mutant lineage (always half the concentration that most recently produced growth). A 1/200 dilution was used to inoculate the next day's evolution plate, and the process was repeated for a total of 8 days of selection. On the final day of evolution all strains were stocked in 30 percent glycerol. Strains were then plated on a pure BHI plate and a single colony was selected for IC_{50} determination. In the case of linezolid mutants, days 2, 4, and 6 were also stocked for further testing.

C. Measuring Drug Resistance and Sensitivity

Experiments to estimate IC_{50} were performed in replicate in 96-well plates by exposing mutants to a drug gradient consisting of 6-14 points–one per well–typically in a linear dilution series prepared in BHI medium with a total volume of 205 uL (200 uL of BHI, 5 uL of 1.5OD cells) per well. After 20 hours of growth the optical density at 600 nm (OD600) was measured using an Enspire Multimodal Plate Reader (Perkin Elmer). This process was repeated for

TABLE I. Table of antibiotics used in this study and their targets.

Drug Name (abbreviation)	**Drug Class**	**Mechanism of Action**
Daptomycin (Dap)	Lipopeptide	Cell membrane insertion
Ampicillin (Amp)	B-lactam	Inhibits cell wall synthesis
Oxacillin (Ox)	B-lactam	Inhibits cell wall synthesis
Ceftriaxone (Cef)	B-lactam	Inhibits cell wall synthesis
Fosfomycin (Fos)	Fosfomycin	Inhibits cell wall synthesis
Tetracycline (Tet)	Tetracycline	30S protein synthesis inhibitor
Docycycline (Dox)	Tetracycline	30S protein synthesis inhibitor
Tigecycline (Tig)	Tetracycline	30S protein synthesis inhibitor
Spectinomycin (Spc)	Aminoglycosides	30S protein synthesis inhibitor
Linezolid (Lin)	Oxazolidinone	50S protein synthesis inhibitor
Chloramphenicol (Cam)	Amphenicol	50S protein synthesis inhibitor
Ciprofloxacin (Cip)	Quinolone	DNA gyrase inhibitor
Levofloxacin (Lev)	Quinolone	DNA gyrase inhibitor
Nitrofurantoin (Nit)	Nitrofuran	Multiple mechanisms
Rifampicin (Rif)	Rifamycin	RNA polymerase inhibitor

all 60 mutants as well as the wild-type, which was measured in replicates of 8.

The optical density (OD600) measurements for each drug concentration were normalized by the OD600 in the absence of drug. To quantify drug resistance, the resulting dose response curve was fit to a Hill-like function $f(x) = (1 + (x/K)^h)^{-1}$ using nonlinear least squares fitting, where K is the half-maximal inhibitory concentration (IC_{50}) and h is a Hill coefficient describing the steepness of the dose-response relationship. A mutant strain was deemed collaterally sensitive (resistant) to an antibiotic if its IC_{50} decreased (increased) by more than $3\sigma_{WT}$, where σ_{WT} is the uncertainty (standard error across replicates) of the IC_{50} measured in the wild-type strain.

D. Hierarchical clustering

Hierarchical clustering was performed in Matlab using, as input, the collateral profiles $\bar{C}$ for each mutant. The distance between each pair of mutants was calculated using a correlation metric (Matlab function pdist with parameter 'correlation'), and the linkage criteria was chosen to be the mean average linkage clustering.

E. Markov decision process (MDP) model

The MDP problem was solved using standard algorithms for MDP models. Briefly, the optimization was performed by first computing the optimal value (or cost) function–the optimal value (cost) corresponding to each state–using the well-established value iteration algorithm[53]. Given the optimal value (cost) function, the optimal policy is then given by the action that minimizes the optimal value (cost) function at the next time step.

REFERENCES

[1]Boucher, H. W., Talbot, G. H., Bradley, J., Edwards, J. E., Gilbert, D., Rice, L. B., Scheld, M., Spellberg, B., and Bartlett, J., "Bad bugs, no drugs; no esape! an update from the infections diseases society of america.," *Clin. Infect. Dis.* **48**, 1–12 (2009).

[2]Goldberg, D. E., Siliciana, R., and Jr, W. R. J., "Outwitting evolution: Fighting drug-resistant tb, malaria, and hiv.," *Cell* **148**, 1271–1283 (2012).

[3]Pfaller, A., "Antifungal drug resistance: Mechanisms, epidemiology, and consequences for treatment.," *Am. J. Med.* **125**, S3–S13 (2012).

[4]Raviglione, M., Marais, B., Floyd, K., Lonnoroth, K., Getahun, H., Migliori, G. B., Harries, A. D., Nunn, P., Lienhardt, C., Graham, S., Hakaya, J., Weyer, K., Cole, S., Kaufmann, S. H. E., and Zumla, A., "Scaling up interentions to achieve global tuberculosis control: Progress and new developments.," *Lancet* **379**, 1902–1913 (2012).

[5]Borst, P., "Cancer drug pan-resistance: Pumps, cancer stem cells, quiescence, epithelial to mesenchymal transition, blocked cell death pathways, persister or what?.," *Open Biol.* **2** (2012).

[6]Pluchino, K. M., Hall, M. D., Goldsborough, A. S., Callaghan, R., and Gotesman, M. M., "Collateral sensitivity as a strategy against cancer multidrug resistance.," *Drug Resis. Updat.* **15**, 98–105 (2012).

[7]Martin, R., "Optimal control drug scheduling of cancer chemotherapy.," *Journal of Antimicrobial Chemotherapy* **28**, 1113–1123 (1992).

[8]Hansen, E., Woods, R. J., and Read, A. F., "How to use a chemotherapeutic agent when resistance to it threatens the patient," *PLoS biology* **15**(2), e2001110 (2017).

[9]Fischer, A., Vázquez-García, I., and Mustonen, V., "The value of monitoring to control evolving populations," *Proceedings of the National Academy of Sciences* **112**(4), 1007–1012 (2015).

[10]Feazel, L. M., Malhotra, A., Perencevich, E. N., Kaboli, P., Diekemea, D. J., and Schweizer, M. L., "Effect of antibiotic stewardship programmes on *clostridium difficile* incidence: a systematic review and meta-analysis.," *Journal of Antimicrobial Chemotherapy* **69**, 1748–1754 (2014).

[11]Smith, D. L., Levin, S. A., and Laxminarayan, R., "Strategic interactions in multi-institutional epidemics of antibiotic resistance.," *Proc. Natl. Acad. Sci. USA* **102**, 3153–3158 (2004).

[12]Bergstrom, C. T., Lo, M., and Lipsitch, M., "Ecological theory suggests that antimicrobial cycling will not reduce antimicrobial resistance in hospitals.," *Proc. Natl. Acad. Sci. USA* **101**, 13285–13290 (2004).

[13]Brown, E. M. and Nathwani, D., "Antibiotic cycling or rotation: a systemic review of the evidence of efficacy.," *Journal of Antimicrobial Chemotherapy* **55**, 6–9 (2005).

[14]Nichol, D., Jeavons, P., Fletcher, A. G., Bonomo, R. A., Maini, P. K., Paul, J. L., Gatenby, R. A., Anderson, A. R., and Scott, J. G., "Steering evolution with sequential therapy to prevent the emergence of bacterial antibiotic resistance," *PLoS computational biology* **11**(9), e1004493 (2015).

[15]Baym, M., Lieberman, T. D., Kelsic, E. D., Chait, R., Gross, R., Yelin, I., and Kishony, R., "Spatiotemporal microbial evolution on antibiotic landscapes," *Science* **353**(6304), 1147–1151 (2016).

[16]Zhang, Q., Lambert, G., Liao, D., Kim, H., Robin, K., Tung, C.-k., Pourmand, N., and Austin, R. H., "Acceleration of emergence of bacterial antibiotic resistance in connected microenvironments," *Science* **333**(6050), 1764–1767 (2011).

[17]Yurtsev, E. A., Chao, H. X., Datta, M. S., Artemova, T., and Gore, J., "Bacterial cheating drives the population dynamics of cooperative antibiotic resistance plasmids," *Molecular systems biology* **9**(1), 683 (2013).

[18]Meredith, H. R., Lopatkin, A. J., Anderson, D. J., and You, L., "Bacterial temporal dynamics enable optimal design of antibiotic treatment," *PLoS computational biology* **11**(4), e1004201 (2015).

[19]Meredith, H. R., Srimani, J. K., Lee, A. J., Lopatkin, A. J., and You, L., "Collective antibiotic tolerance: mechanisms, dynamics and intervention," *Nature chemical biology* **11**(3), 182–188 (2015).

[20]Vega, N. M. and Gore, J., "Collective antibiotic resistance: mechanisms and implications," *Current opinion in microbiology* **21**, 28–34 (2014).

[21]Balaban, N. Q., Merrin, J., Chait, R., Kowalik, L., and Leibler, S., "Bacterial persistence as a phenotypic switch," *Science* **305**(5690), 1622–1625 (2004).

[22]Tan, C., Smith, R. P., Srimani, J. K., Riccione, K. A., Prasada, S., Kuehn, M., and You, L., "The inoculum effect and band-pass bacterial response to periodic antibiotic treatment," *Molecular systems biology* **8**(1), 617 (2012).

[23]Karslake, J., Maltas, J., Brumm, P., and Wood, K. B., "Population density modulates drug inhibition and gives rise to potential bistability of treatment outcomes for bacterial infections," *PLoS computational biology* **12**(10), e1005098 (2016).

[24]Torella, J. P., Chait, R., and Kishony, R., "Optimal drug synergy in antimicrobial treatments.," *PlOS Comput. Biol.*. **6** (2010).

[25]Michel, J., Yeh, P. J., Chait, R., Jr, R. C. M., and Kishony, R., "Drug interactions modulate the potential for evolution of resistance.," *Proc. Natl. Acad. Sci. USA* **105**, 14918–14923 (2008).

[26]Hegreness, M., Shoresh, N., Damian, D., Hartl, D., and Kishony, R., "Accelerated evolution of resistance in multi-drug environments.," *Proc. Natl. Acad. Sci. USA* **105**, 13977–13981 (2008).

[27]Chait, R., Craney, A., and Kishony, R., "Antibiotic interactions that select against resistance," *Nature* **446**(7136), 668 (2007).

[28]Baym, M., Stone, L. K., and Kishony, R., "Multidrug evolutionary strategies to reverse antibiotic resistance," *Science* **351**(6268), aad3292 (2016).

[29]Wood, K., Nishida, S., Sontag, E. D., and Cluzel, P., "Mechanism-independent method for predicting response to multidrug combinations in bacteria," *Proceedings of the National Academy of Sciences* **109**(30), 12254–12259 (2012).

[30]Zimmer, A., Katzir, I., Dekel, E., Mayo, A. E., and Alon, U., "Prediction of multidimensional drug dose responses based on measurements of drug pairs," *Proceedings of the National Academy of Sciences* **113**(37), 10442–10447 (2016).

[31]Zimmer, A., Tendler, A., Katzir, I., Mayo, A., and Alon, U., "Prediction of drug cocktail effects when the number of measurements is limited," *PLoS biology* **15**(10), e2002518 (2017).

[32]de Evgrafov, M. R., Gumpert, H., Munck, C., Thomsen, T. T., and Sommer, M. O. A., "Collateral resistance and sensitivity modulate evolution in high-level resistance to drug combination treatment in *staphylococcus aureus.*," *Mol. Biol. Evol.* **32**, 1175–1185 (2015).

[33]Oz, T., Guvenek, A., Yildiz, S., Karaboga, E., Tamer, Y. T., Mumcuyan, N., Ozan, V. B., Senturk, G. H., Cokol, M., Yeh, P., and Toprak, E., "Strength of selection pressure is an important parameter contributing to the complexity of antibiotic resistance evolution.," *Mol. Biol. Evol.* **31**, 2387–2401 (2014).

[34]Lazar, V., Nagy, I., Spohn, R., Csorgo, B., Gyorkei, A., Nyerges, A., Horvath, B., Voros, A., Busa-Fekete, R., Hrtyan, M., Bogos, B., Mehi, O., Fekete, G., Szappanos, B., Kegl, B., Papp, B., and Pal, C., "Genome-wide analysis captures the determinants of the antibiotic cross-resistance interaction network.," *Nat. Commun.* **5** (2014).

[35]Lazar, V., Singh, G. P., Spohn, R., Nagy, I., Horvath, B., Hrtyan, M., Busa-Fekete, R., Bogos, B., Mehi, O., Csorgo, B., Posfai, G., Fekete, G., Szappanos, B., Kegl, B., Papp, B., and Pal, C., "Bacterial evolution and antibiotic hypersensitivity.," *Mol. Syst. Biol.* **9** (2013).

[36]Shoval, O., Sheftel, H., Shinar, G., Hart, Y., Ramote, O., Mayo, A., Dekel, E., Kavanagh, K., and Alon, U., "Evolutionary trade-offs, pareto optimality, and the geometry of phenotype space," *Science* **336**(6085), 1157–1160 (2012).

[37]Hart, Y., Sheftel, H., Hausser, J., Szekely, P., Ben-Moshe, N. B., Korem, Y., Tendler, A., Mayo, A. E., and Alon, U., "Inferring biological tasks using pareto analysis of high-dimensional data," *Nature methods* **12**(3), 233–235 (2015).

[38]Imamovic, L. and Sommer, M. O. A., "Use of collateral sensitivity networks to design drug cycling protocols that avoid resistance development.," *Sci. Transl. Med* **5**, 204ra132

(2013).

[39]Kim, S., Lieberman, T. D., and Kishony, R., "Alternating antibiotic treatments constrain evolutionary paths to multidrug resistance.," *Proc. Natl. Acad. Sci. USA* **111**, 1449414499 (2014).

[40]Yoshida, M., Reyes, S. G., Tsudo, S., Horinouchi, T., Furusawa, C., and Cronin, L., "Time-programmable dosing allows the manipulation, suppression and reversal of antibiotic drug resistance *in vitro*.," *Nat. Commun.* **8** (2017).

[41]Munck, C., Gumpert, H. K., Wallin, A. I. N., Wang, H. H., and Sommer, M. O. A., "Prediction of resistance development against drug components by collateral responses to component drugs.," *Sci. Transl. Med* **6**, 262ra156 (2014).

[42]Barbosa, C., Trebosc, V., Kemmer, C., Rosenstiel, P., Beardmore, R., Schulenburg, H., and Jansen, G., "Alternative evolutionary paths to bacterial antibiotic resistance cause distinct collateral effects.," *Mol. Biol. Evol.* **34**, 22292244 (2017).

[43]Dhawan, A., Nichol, D., Kinose, F., Abazeed, M. E., Marusyk, A., Haura, E. B., and Scott, J. G., "Collateral sensitivity networks reveal evolutionary instability and novel treatment strategies in alk mutated non-small cell lung cancer," *Scientific Reports* **7** (2017).

[44]Nichol, D., Rutter, J., Bryant, C., Jeavons, P., Anderson, A., Bonomo, R., and Scott, J., "Collateral sensitivity is contingent on the repeatability of evolution," *bioRxiv* (2017).

[45]Clewell, D. B., Gilmore, M. S., Ike, Y., and Shankar, N., [*Enterococci: from commensals to leading causes of drug resistant infection*], Massachusetts Eye and Ear Infirmary (2014).

[46]Donlan, R. M., "Biofilms and device-associated infections.," *Emerging infectious diseases* **7**(2), 277 (2001).

[47]O'Driscoll, T. and Crank, C. W., "Vancomycin-resistant enterococcal infections: epidemiology, clinical manifestations and optimal management.," *Drug Resis. Updat.* **8**, 217–230 (2015).

[48]Cetinkaya, Y., Falk, P., and Mayhall, C. G., "Vancomycin resistant enterococci.," *Clin. Microbiol. Rev.* **13**, 686–707 (2000).

[49]Kelesidis, T., Humphries, R., Uslan, D. Z., and Pegues, D. A., "Daptomycin nonsusceptible enterococci: an emerging challenge for clinicians," *Clinical Infectious Diseases* **52**(2), 228–234 (2011).

[50]Tran, T. T., Munita, J. M., and Arias, C. A., "Mechanisms of drug resistance: daptomycin resistance," *Annals of the New York Academy of Sciences* **1354**(1), 32–53 (2015).

[51]Zhao, B., Sedlak, J. C., Srinivas, R., Creixell, P., Pritchard, J. R., Tidor, B., Lauffenburger, D. A., and Hemann, M. T., "Exploiting temporal collateral sensitivity in tumor clonal evolution.," *Cell.* **165**, 1–13 (2016).

[52]Yeh, P., Tschumi, A. I., and Kishony, R., "Functional classification of drugs by properties of their pairwise interactions.," *Nature Genetics* **38**, 489–494 (2006).

[53]Feinberg, E. A. and Shwartz, A., [*Handbook of Markov decision processes: methods and applications*], vol. 40, Springer Science & Business Media (2012).

[54]Humphries, R. M., Pollett, S., and Sakoulas, G., "A current perspective on daptomycin for the clinical microbiologist.," *Clin. Microbiol. Rev.* **26**, 759–780 (2013).

[55]Yu, W., Hallinen, K. M., and Wood, K. B., "Interplay between antibiotic efficacy and drug-induced lysis underlies enhanced biofilm formation at subinhibitory drug concentrations," *Antimicrobial agents and chemotherapy* **62**(1), e01603–17 (2018).

[56]Martin, M., Hölscher, T., Dragoš, A., Cooper, V. S., and Kovács, Á. T., "Laboratory evolution of microbial interactions in bacterial biofilms," *Journal of bacteriology* **198**(19), 2564–2571 (2016).

[57]Steenackers, H. P., Parijs, I., Foster, K. R., and Vanderleyden, J., "Experimental evolution in biofilm populations," *FEMS microbiology reviews* **40**(3), 373–397 (2016).

[58]Sahm, D. F., Kissinger, J., Gilmore, M. S., Murray, P. R., Mulder, R., Solliday, J., and Clarke, B., "In vitro susceptibility studies of vancomycin-resistant enterococcus faecalis," *Antimicrobial Agents and Chemotherapy* **33**, 1588–1591 (Sept. 1989).